# Water Channel of Horseradish Peroxidase Studied by the Charge-Transfer Absorption Band of Ferric Heme†

**B. Zelent,‡ A. D. Kaposi,§ N. V. Nucci,‡ K. A. Sharp,‡ S. D. Dalosto,‡ W. W. Wright,‡ and J. M. Vanderkooi*,‡**

*Department of Biochemistry and Biophysics, School of Medicine, University of Pennsylvania, Philadelphia, Pennsylvania 19104, and Department of Biophysics and Radiation Biology, Semmelweis University of Medicine, H-1444 P.O.B. 263, Budapest, Hungary*

*Received: December 1, 2003; In Final Form: March 4, 2004*

The heme of horseradish peroxidase is buried in the protein, but a channel from the protein surface connects the aqueous solution to the heme site. Ferric horseradish peroxidase has an absorption band at 640 nm that is attributed to a charge-transfer (CT) transition between the $a_{2u}$ HOMO of $\pi$ electrons of the porphyrin ring and the $d_{xy}/d_{yz}$ orbital of the ferric ion. Because the water channel extends to the Fe, it seems likely that the CT band will be sensitive to the hydration of the protein. To study this premise, the protein was incorporated into trehalose/sucrose glasses and the hydration of the sugar glasses was varied. Absorption spectra of HRP in sugar glasses and in glycerol/water were taken in the range 10−300 K. The CT absorption band shows vibronic fine structure. The peak positions are the same in hydrated sugar and glycerol/water but the peak positions change in desiccated sugar glass. The data suggest that in hydrated, but not desiccated, sugar glass, water is retained in the heme pocket. Binding of the competitive inhibitor benzohydroxamic acid to the protein increases the CT absorption and resolution. The effect of benzohydroxamic acid on the Fe as calculated using a combination of density functional theory and molecular mechanics is to stabilize the spin state $^3/_2$ with respect to $^5/_2$. At low temperature the widths of the lines in the CT band are narrower for the protein in glycerol/water (glass transition at ∼150 K) than in trehalose/sucrose (glass formation at 65 °C). This indicates that the CT band is inhomogeneously broadened and sensitive to the solvent. The spectral narrowing of the CT absorption occurs as the temperature decreases over the temperature range studied. Water, as indicated by the OH stretch, also shifts in this range. The findings are discussed in terms of how buried water and nearby charges can modulate the activity of the heme.

## Introduction

Biological structures are bathed in water. Channels in biological macromolecules and membranes allow for the penetration of small ions and water across membranes and within proteins. For the channel to be effective, it should permit the selective permeation of the desired substance, and it should have a means to control the access. In this paper, we are addressing the question of how exterior solvent conditions influence a group in the interior using horseradish peroxidase (HRP) as a model. Peroxidases are heme-containing proteins that catalyze the sequential one-electron reduction of $H_2O_2$ to water.[1] The reaction catalyzed by HRP follows this sequence:

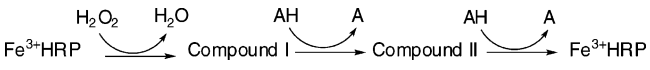


where AH is an aromatic H-donor reductant. Adding $H_2O_2$ to the resting enzyme produces a ferryl compound at the heme, called compound I. In the crystal structure of horseradish peroxidase, a channel is apparent from the surface to the heme; this channel allows for the infiltration of the substrate, $H_2O_2$, and the release of the product, $H_2O$.[2] The next step is the binding of the substrate AH. A competitive inhibitor benzohydroxamic acid (BHA) binds with high affinity at the site where AH binds.[3,4]

The heme and relevant residues of HRP are shown in Figure 1. Figure 1a shows the electrostatic potential of the protein surface with a cut-out view that allows the heme, Asp70, His42, Arg38, and Phe68 to be seen. In this slice of the heme pocket, the pore is seen as that part of the surface that extends to the heme. When BHA binds, as depicted in Figure 1b, it plugs the pore and there is a conformational change that includes the flipping of Phe68.[5] The net result is that the solvent access to the heme becomes restricted. Physical measurements bear out this picture. For a metal derivative of HRP, the accessibility of oxygen to the porphyrin is greatly reduced when BHA binds, consistent with the view that its binding closes the channel that provides access to the surface.[6]

Heme proteins have intense visible absorption bands that arise predominantly from transitions of the electrons of the porphyrin ring but also have contributions of the iron and its ligands.[7] The visible absorption spectrum of high-spin ferric hemes has a pronounced absorption band at >600 nm. This band is polarized in the *z* direction,[8] and it is attributed to a charge-transfer (CT) transition from the $a_{2u}$ HOMO of the heme to the $d_{xy}/d_{yz}$ orbital of the metal.[8] Earlier it was recognized that the charge-transfer absorption band is enhanced when the symmetry of the heme is broken from $D_{4h}$ such that electron density at the metal and porphyrin changes.[9] Packing forces of the polypeptide chain can distort the heme from planarity.[10] Local

† Part of the special issue "Gerald Small Festschrift".

* Corresponding author. E-mail: vanderko@mail.med.upenn.edu. Phone: 215-898-8783.

‡ University of Pennsylvania.

§ Semmelweis University.

10.1021/jp037664q CCC: $27.50 
Published on Web 05/08/2004

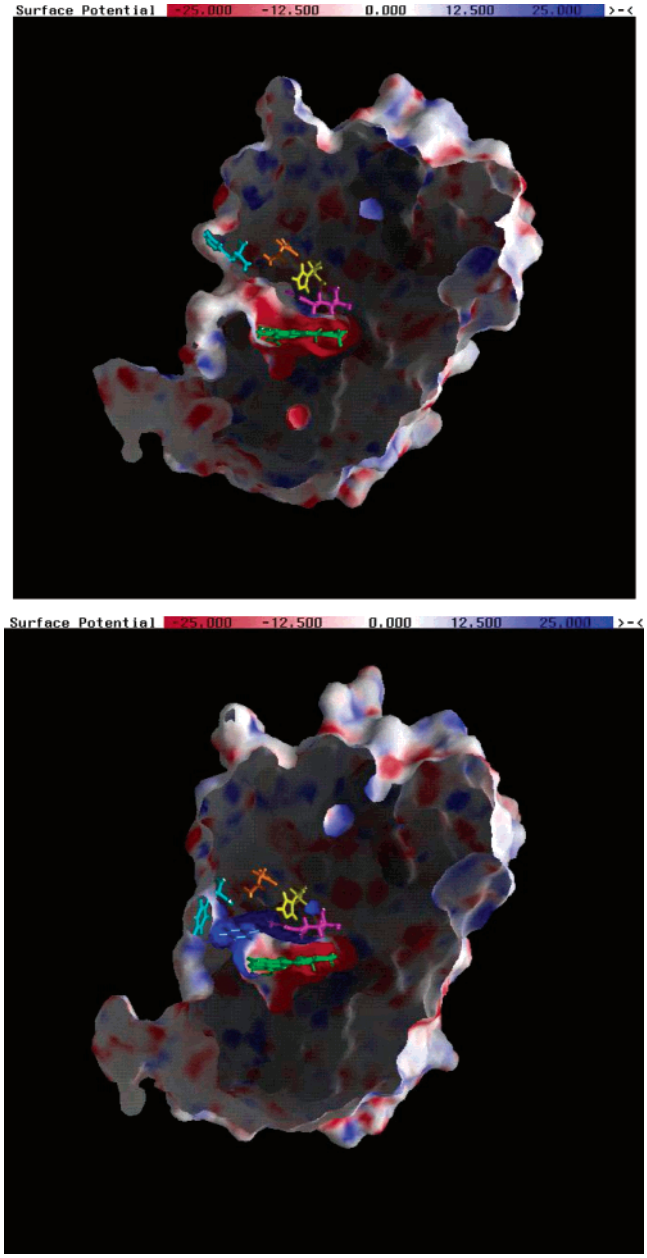


**Figure 1.** Model of the heme pocket and protein surface of HRP. Top: no BHA, coordinates from PDB 1ATJ. Bottom: with BHA, coordinates from PDB 2ATJ. The heme is green, Asp70 is orange, His42 is yellow, Arg38 is magenta, Phe68 is cyan, and BHA is dark blue.

electric fields and ring substituents also reduce the symmetry of the heme.[11−14] This reduction of symmetry can change the interactions of the $d_\pi$ orbitals of the metal with the $\pi$ orbitals of the pyrrole rings. The metal $d_\pi$ electrons can also be raised in energy by interaction with the axial ligands. Due to the sensitivity of the charge-transfer transition to various influences of the protein the CT absorption band can be used to study subtle properties of the heme site.[15−17]

The question that is addressed in this paper is how the solvent communicates with the protein center. We make use of the CT absorption band as a spectroscopic marker by comparing the CT absorption of the resting ferric protein in glycerol/water and in trehalose−sucrose (TS) glass as a function of temperature. Glycerol/water is a commonly used laboratory cryosolvent,[18] whereas a wide interest in protein interactions with sugars arises because many species use sugars to protect against heat, cold, and dehydration.[19] Sugar glasses provide the investigator with a means to immobilize proteins at ambient temperatures and then to study proteins over a large temperature range.[14,20−23] The water content in the sugar glass can be changed by equilibrating the glass in an atmosphere of known humidity.[24] We here show that the hydration conditions affect the CT band. In contrast, when the enzyme is in the presence of the substrate analogue BHA, the iron active site appears to be occluded from the matrix water, as indicated by the independence of the spectra on the hydration of the matrix.

## Materials and Methods

**Materials.** Water was deionized and then glass distilled. Horseradish peroxidase type III (isoenzyme C), glycerol 99% (GC), D-8 glycerol, D(+)-trehalose (α-D-glucopyranosyl-α-D-glucopyranoside), sucrose (α-D-glucopyranosyl-β-D-fructopyranoside) and benzohydroxamic acid were obtained from Sigma Chemical Co. (St. Louis, MO). The horseradish peroxidase was purified using column chromatography based upon the procedure of Paul.[25] HRP (100 mg) was applied to a carboxymethyl cellulose CM-52 (Whatman Ltd, Maidstone, England) column equilibrated with 0.005 M Tris buffer at pH 7.4. The fractions of protein solution were checked for the Reinheitzahl (RZ) value (ratio of absorbances at 402 and 280 nm) using an absorption spectrophotometer (Hitachi Perkin-Elmer U-3000). The fractions of HRP solution with the RZ ≥ 3.1 were collected and lyophilized.

**Sugar Glass Formation.** Solid and stable sugar glasses are formed when a mixture of sugars is used in their preparation.[26] Trehalose (1.2 g) and sucrose (1.2 g) were dissolved in 2 mL of distilled water to form the stock sugar solution. The sugar glass was prepared as follows. For UV/vis measurements, 4 mg of HRP was dissolved in 350 μL of 0.1 M $PO_4$ buffer + 100 μL of stock sugar solution (with or without 4 μL of 70 mM BHA in absolute ethanol) and the pH was adjusted to 6.0. Following this, the protein sample was placed onto a 25 mm round quartz plate of 2 mm thickness (Escoproducts, Oak Ridge, NJ). The quartz disk with the sample was placed on a VWR Scientific Products Heat Block at 65 °C for ∼2 h until dry. The resulting sugar glass was hard to the touch and optically clear.

To obtain the *wet* sample, the *dry* sugar sample was exposed at 20 °C for 2 h to air with 65% relative humidity. This humidity was achieved placing the sample in a closed container containing a saturated solution of ammonium nitrate. In the wet sample, the water to sugar molar ratio is ∼2. In the dry sample this ratio is about 0.1.[24]

**Cryosolution Preparation.** The solution used for cryogenic measurements was 60/40% v/v glycerol/ aqueous buffer. For UV/vis absorption measurements, 6 mg of lyophilized HRP was dissolved in 60 μL of glycerol + 40 μL 0.1 M $PO_4$ buffer (with or without 4 μL of 70 mM BHA in absolute ethanol) and the pH was adjusted to 6.0. The solution was placed between two circular quartz plates with a 200 μm Teflon spacer.

**Spectroscopy**. A Hitachi Perkin-Elmer U-3000 spectrophotometer was used to take visible absorption spectra with spectral resolution of 1 nm. The temperature of the sample was maintained using an APD closed cycle Helitran cryostat (Advanced Research Systems, Allentown, PA). The cryostat sample chamber was filled with He gas at atmospheric pressure, which aids in the transfer of heat from the sample. The outer cryostat windows were made of quartz and the inner windows, which experience the temperature gradient, were made of sapphire. The temperature was measured with a silicon diode near the sample, and the temperature was controlled using a Model 9650

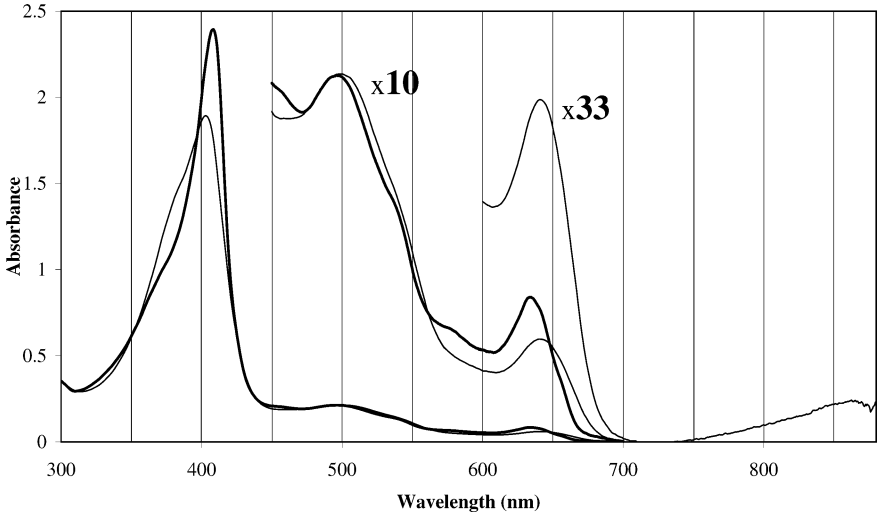


**Figure 2.** Absorption spectra of HRP in glycerol/water (60/40, v/v) at pH 6 measured at 295 K (thin lines) and 90 K (thick lines).

temperature controller (Scientific Instruments, Palm Beach, FL). The spectra were obtained in sequence from high temperature to low temperature at 10 deg increments starting at 290 K, except for the lowest temperature, which was 11−17 K. The rate of cooling was 1−2 deg/min.

Infrared absorption spectra were obtained with a Bruker IFS 66 Fourier transform IR spectrophotometer (Bruker, Brookline, MA). The sample compartment was purged with nitrogen to reduce the contribution from water vapor, and light levels were monitored using an HgCdTe (MCT) detector. The spectral resolution was 2 $cm^{-1}$. All spectra were taken in the transmission mode and transformed to absorption. The spectra were smoothed using a Savitsky−Golay smoothing algorithm over 9 points. The same Helitran cryostat described above was used for IR measurements, except in this case windows of $CaF_2$ were used on the outer cryostat. The inner cryostat windows were 2 mm thick and were made of ZnSe (Janos Technology, Townshend, VT).

The spectra were analyzed for their components using the PeakFit Program (Jandel Scientific Software, San Rafael, CA). A Gaussian function in the form

$$a_0 \exp\left[-0.5\left(\frac{x-a_1}{a_2}\right)^2\right]$$

where $a_0$, $a_1$, and $a_2$ denote amplitude, maximal position, and widths, respectively, was used for deconvolution of the peaks.

**Structure Analysis and Electrostatic Surface Mapping.** The structures used were 1ATJ and 2ATJ and HRP alone and complexed with BHA, respectively. Electrostatic potentials were calculated with the finite difference solutions to the Poisson−Boltzmann equation[27] as implemented in the *DelPhi* software package.[28,29] Images were created using *GRASP*.[30] Electrostatic potentials were displayed with the standard color code, and structures were cut away to display the heme and relevant amino acids.

**Calculated Effects of the Protein on Spin State and Distances.** The beginning structures were taken from the Protein Data Base PDB 1ATJ for HRP without BHA and 2ATJ for HRP with bound BHA. The heme with all its substituents, on the proximal side histidine, His170 and Asp247 and on the distal side a water molecule and His42 were included in the quantum mechanic part of the calculation. In the calculations where BHA is present, BHA was also included in the quantum mechanic component. The amino acids were modeled by their side chain according with the standard options of Qsite to build the quantum mechanics models. All crystallographic waters were conserved. We used density functional calculations with the hybrid density functional B3LYP (RODFT) together with the polarized basis sets LACVP** for Fe and 6-31G for the rest of the atoms in the quantum mechanic part.[31] The OPLS-AA MM force field was used in the molecular mechanic part. In this way all the atoms in the QM part feel the electrostatic field generated by the molecular mechanics calculation.

All the calculations were performed using the standard options in the Qsite program package (Qsite, Schrodinger, Inc., Portland OR and IMPACT, Schrodinger, Inc., Portland, OR). The structures were completely relaxed without constraints until the total energy fell below a threshold of $5 \times 10^{-5}$ au.

## Results

**Absorption Spectrum of HRP.** The electronic absorption spectrum of HRP in glycerol/water was taken at high and low temperature at pH 6.0 in the absence of BHA (Figure 2) and in the presence of BHA (Figure 3). The spectra at room temperature are comparable to what has been reported previously.[32] We include them to point out several features. At low temperature, HRP in the absence of BHA shows sharpening of the Soret peak at 402 nm. The Soret peak in the presence of BHA does not show a detectable change with temperature, consistent with the conversion of the iron to high spin, and 6-coordination at all temperatures.[33−35] The absorption bands of HRP in the visible region, from ∼450 to ∼550 nm and the band at 870 nm show a relatively small change in position with temperature. In contrast, the CT absorption band, ∼600−680 nm, shows quite a pronounced shift and sharpening of the band leading to vibronic resolution at low temperature. The intensity of the CT absorption band for HRP increases in the presence of BHA. This is apparent in the ratio of absorbance for the CT band/visible absorption given in Table 1. In the presence of BHA, the CT band of HRP at room temperature shifts to lower wavelength as compared to the position of the band in the absence of BHA. At room temperature neither band had spectral fine-structure.

**CT Absorption of HRP.** The absorption spectrum in the CT region of HRP was examined in more detail. Spectra are shown at various temperatures for HRP at pH 6.0 in glycerol/water (Figure 4), in hydrated TS (Figure 5), and in desiccated sugar glass (Figure 6). The spectra are overlaid for the higher

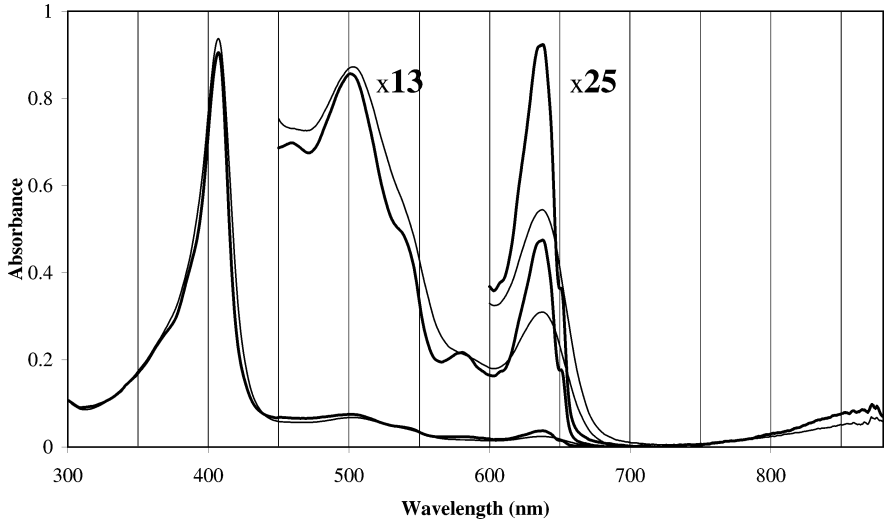


**Figure 3.** Absorption spectra of HRP with BHA in glycerol/water (60/40, v/v) at pH 6 measured at 295 K (thin lines) and 11 K (thick lines).

**TABLE 1: Positions and Widths of the CT Absorption Band of HRP at Room Temperature in Glycerol/Water (GW) and Sugar Glass (TS) at pH 6**

| protein | matrix | peak center, nm | width, fwhm, nm | $A_{CT}/A_{\alpha}$ | wavelengths[a] |
|---|---|---|---|---|---|
| HRP | GW | 642.7 | 43.9 | 0.28 | 641/500 |
| | TS wet | 639.1 | 45.6 | 0.30 | 638/500 |
| | TS dry | 646.7 | 42.3 | 0.28 | 646/500 |
| HRP + BHA | GW | 638.1 | 38.5 | 0.36 | 638/503 |
| | TS wet | 637.6 | 38.9 | 0.38 | 637/503 |
| | TS dry | 638.3 | 38.7 | 0.36 | 638/503 |

[a] Wavelengths indicate the wavelengths that were used to determine the absorbance ratios: $A_{CT}/A_{\alpha}$. GW refers to the glycerol/water cryosolvent, and TS refers to trehalose/sucrose glass, prepared as described in Materials and Methods.

temperatures and, for clarity, are off-set at the lowest temperatures. The stacked spectra emphasize that at low temperature, the CT absorption has vibronic resolution. The resolution is higher for the glycerol/water than for hydrated TS, but the overall spectral positions are the same. At the higher temperatures, the overlaid spectra reveal a continuous decrease in bandwidth as the temperature decreases. The spectra for HRP in hydrated (wet) and desiccated (dry) sugar glass appear the same at room temperature, but at low-temperature details are different. For the HRP in desiccated sugar glass, the spectrum has more of the longer wavelength component, showing that the presence of water influences the spectrum. The Soret peak at low temperature was also affected by the presence of water in the sugar glass. In wet sugar glass, the Soret peak sharpened at low temperature in the same manner as was observed in the glycerol/water solution.

We considered whether the shift in the spectrum could be due to a shift in the p*K* of some group as a function of temperature, and therefore be arising from two protonation states of the protein. Several experiments argue against this. We examined the spectrum of the pH indicator 8-hydroxypyrene-1,3,6-sulfonate, trisodium salt. The protonated/deprotonated ratio did not change over the excursion temperature, indicating that the pH around this group did not change significantly in this solvent as a function of temperature. The more direct test of whether pH changes are responsible for the spectral shifts is to take the spectra of HRP at low and high pH's. We took the spectra of HRP at pH 5.0 and the spectra were the same as for pH 6 (data not shown). This indicates that under our conditions, the sample did not shift to the acidic, protonated form. At high pH the distal

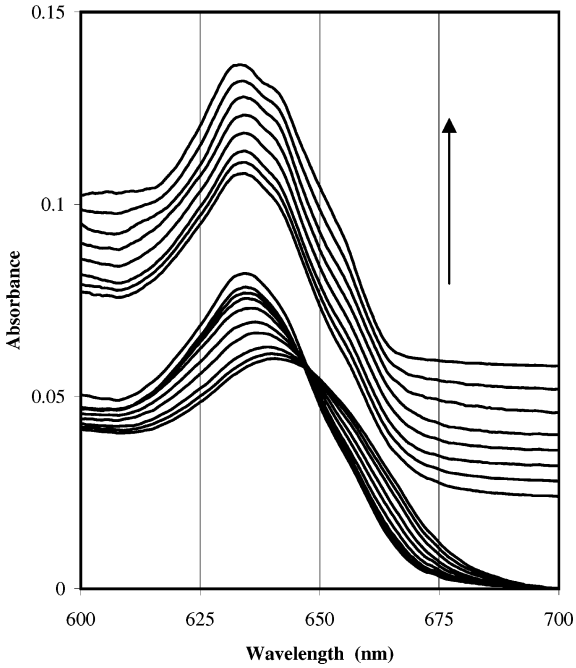


**Figure 4.** CT absorption band of HRP in glycerol/water (60/40, v/v) at pH 6 over a range of temperatures. The temperature was varied from 290 to 110 K in the direction of the arrow in 20 deg increments. The offset spectra were taken at 90, 80, 70, 60, 50, 35, 20, and 13 K, bottom to top. The arrow indicates the sequence the spectra were taken, and points to the lowest temperature.

His becomes deprotonated, and so we also repeated the experiment for the sample in glycerol/water at pH 9.0. The spectra are shown in Figure 7. Again the spectra showed vibronic resolution. The peak positions are distinct from that of Figure 4.

**CT Absorption of HRP with BHA.** Absorption spectra of HRP with bound BHA are shown at low and high temperature in Figure 8 for the sample in glycerol/water. At room temperature, the effect of BHA is comparable to what has been reported.[4] The absorption in the charge-transfer region of the spectrum for the sample in wet sugar glass is shown in Figure 9 and in dry sugar glass in Figure 10. The major difference between the two matrixes is apparent in the spectral resolution, but the peak position remains the same. It should be pointed out that the resolution of the band increases as the temperature decreases, even below the glass transition. This is especially

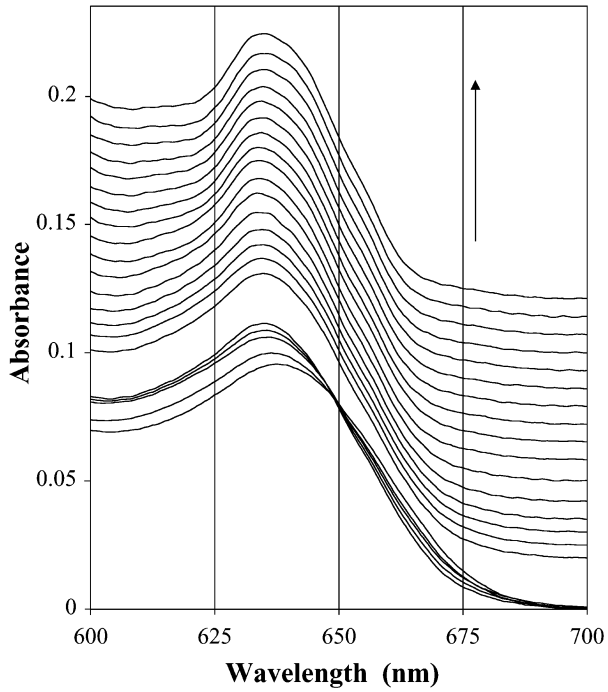


**Figure 5.** CT absorption band of HRP in trehalose/sucrose glass (wet) at pH 6 over a range of temperatures. The temperature was varied from 290 to 210 K in the direction of the arrow in 20 deg increments. The offset spectra were taken at 200, 190, 180, 170, 150, 130, 110, 100, 90, 80, 70, 60, 45, 35, 25, and 15 K, bottom to top. The arrow indicates the sequence the spectra were taken, and points to the lowest temperature.

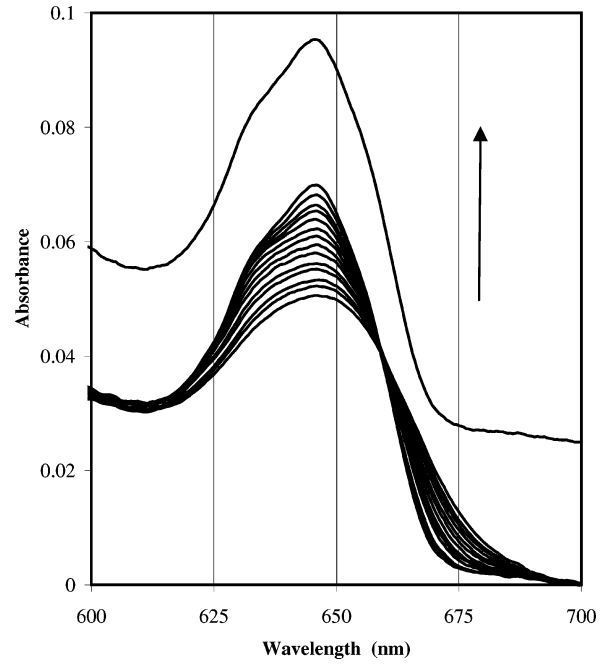


**Figure 6.** CT absorption band of HRP in trehalose/sucrose glass (dry) at pH 6 over a range of temperatures. The temperature was varied from 290 to 30 K in 20 deg increments. The broadest spectra were at the highest temperature; the narrowest were at the lowest temperature. The offset spectrum was taken at 13 K.

evident in Figure 8 for the peak that occurs at 652 nm. As temperature decreases from 60 to 17 K, seen in the offset spectra, this band is narrowing.

**Fitting Parameters for the CT Absorption Band.** The spectra were analyzed for position and line width. Examples of the fits are shown in Figures 11 and 12. There is no measurable

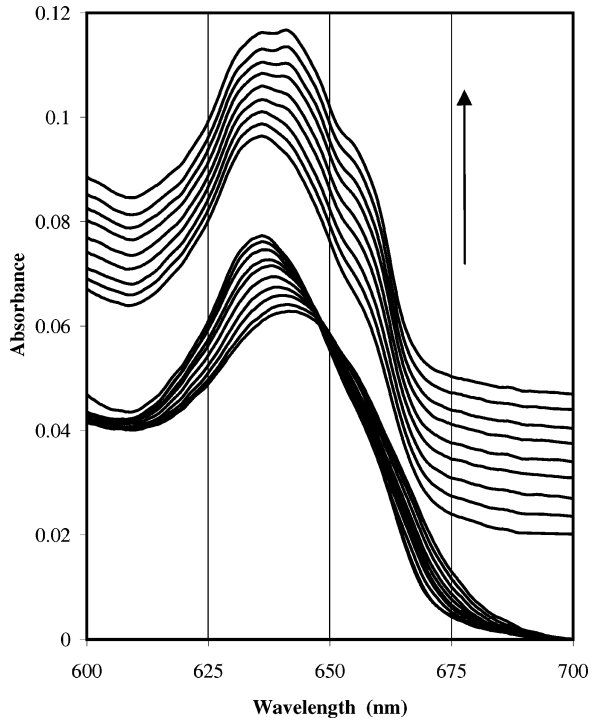


**Figure 7.** CT absorption band of HRP with BHA in glycerol/water (60/40, v/v) at pH 9 over a range of temperatures. The temperature was varied from 290 to 110 K in the direction of the arrow. The temperatures of the offset spectra were 90 to 20 K in 10 deg increments. Top spectrum was at 16 K. The arrow points toward the lowest temperature.

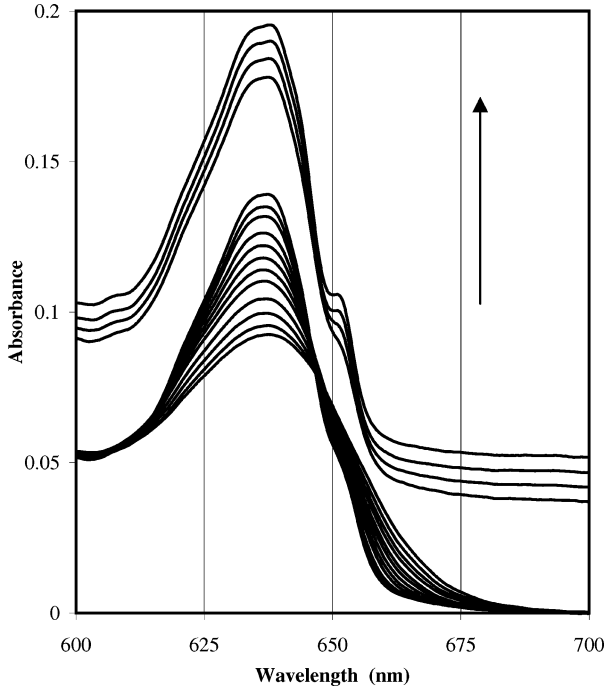


**Figure 8.** CT absorption band of HRP with BHA in glycerol/water (60/40, v/v) at pH 6 over a range of temperatures. The temperature was varied from 290 to 70 K in the direction of the arrow. The temperatures of the offset spectra were 60, 40, 20, and 17 K. Arrow points to the lowest temperature.

difference in positions of peaks but the peak width is measurably narrower with glycerol/water. The values are given in Table 2 for the conditions given in Figures 4−10. The fitting emphasizes that vibronic resolution is seen at low temperature. At room temperature the charge-transfer band shows no resolution; the

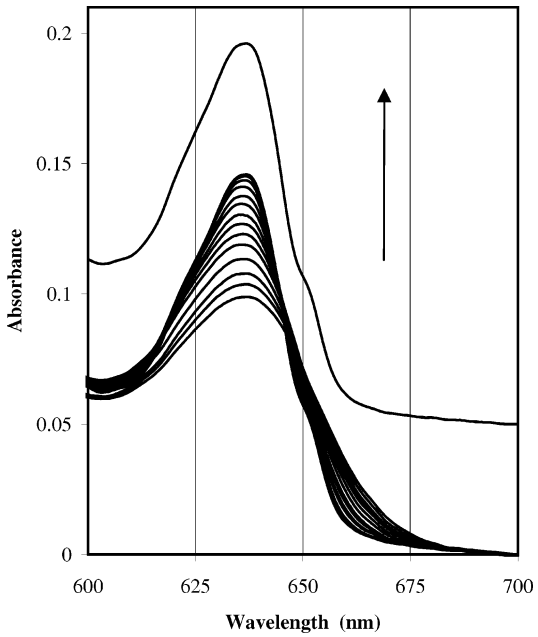


**Figure 9.** CT absorption band of HRP with BHA in trehalose/sucrose glass (wet) at pH 6 over a range of temperatures. The temperature was varied from 290 to 30 K in 20 deg increments. The offset spectrum was taken at 12 K. Arrow points to the lowest temperature.

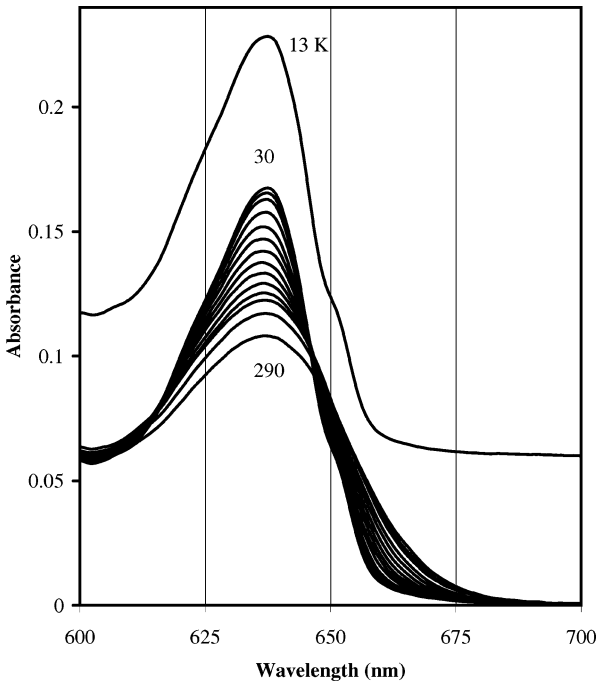


**Figure 10.** CT absorption band of HRP with BHA in trehalose/sucrose glass (dry) at pH 6 over a range of temperatures. The temperature was varied from 290 to 30 K in 20 deg increments. The offset spectrum was taken at 13 K.

band was fit to two Gaussian widths, but this is not a unique fit because one width would also give fits with deviations $r^2 = 0.9998$.

**Infrared Absorption Spectrum in the OH Stretch Region.** In glycerol/water the CT band of HRP in the absence of BHA (Figure 4) and the presence of BHA (Figure 8) show spectral shift and sharpening to about 140−160 K. This temperature is the glass transition of this solvent.[24] But even below the glass transition, there was increased resolution as the temperature decreased. At the same temperature range that these experiments were carried out, the OH stretch of the solvent was monitored

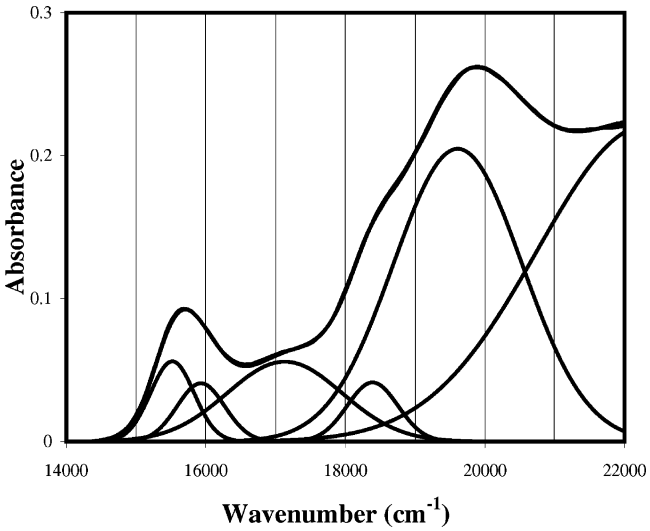


**Figure 11.** Absorption spectrum of HRP with BHA in glycerol/water (60/40, v/v) pH 6 at 295 K. Gaussian function fits had the following respective position and widths (in $cm^{-1}$) and relative amplitudes: 15520, 312, 0.056; 15930, 341, 0.041; 17130, 824, 0.056; 18390, 364, 0.041; 19610, 922, 0.205; and 22320, 11568, 0.221. Top spectra are overlays of experimental spectrum and the sum of deconvolved peaks. Fit $r^2 = 0.9998$.

**TABLE 2: CT Absorption Band of HRP in Glycerol/Water and Sugar Glass at pH 6**

| | | 295 K | | 12−17 K | |
|---|---|---|---|---|---|
| protein | solvent | peak center, $cm^{-1}$ | width, fwhm, $cm^{-1}$ | peak center, $cm^{-1}$ | width, fwhm, $cm^{-1}$ |
| HRP | GW | 15420 | 864 | 15320 | 364 |
| | | 15990 | 950 | 15630 | 506 |
| | | | | 15910 | 486 |
| | | | | 16320 | 752 |
| | TS (wet) | 15510 | 915 | 15320 | 422 |
| | | 16090 | 856 | 15680 | 530 |
| | | | | 15900 | 659 |
| | | | | 16480 | 962 |
| | TS (dry) | 15350 | 818 | 15280 | 418 |
| | | 15860 | 910 | 15570 | 654 |
| | | | | 15960 | 914 |
| HRP + BHA | GW | 15520 | 735 | 15330 | 98 |
| | | 15930 | 803 | 15600 | 331 |
| | | | | 15830 | 534 |
| | | | | 16110 | 1095 |
| | TS (wet) | 15520 | 750 | 15330 | 128 |
| | | 15930 | 558 | 15600 | 319 |
| | | | | 15830 | 520 |
| | | | | 16110 | 1220 |
| | TS (dry) | 15520 | 734 | 15330 | 120 |
| | | 15930 | 754 | 15600 | 336 |
| | | | | 15830 | 555 |
| | | | | 16110 | 1119 |

by infrared absorption. In the experiment given in Figure 13, the OH of residual water in a $D_2O$/ perdeuterated glycerol solution and in the presence of HRP was examined. As seen in the figure the shift in the OH stretch is large until the glass transition, and then there is further shift and sharpening as temperature decreases. Because the proton of the −OH group of glycerol can exchange with the residual water, the OH stretch is arising from DOH and glycerol−OH. Glycerol has two positions for −OH: on the 1 and 2 carbons of the molecule. Therefore, three −OH chemical species exist in the solution. At low temperature, three peaks appear; however, because of the H-bond networks that exist in this solvent it is not clear that these can be assigned to the three species of −OH. The point is that even at the lowest temperatures, the absorption is

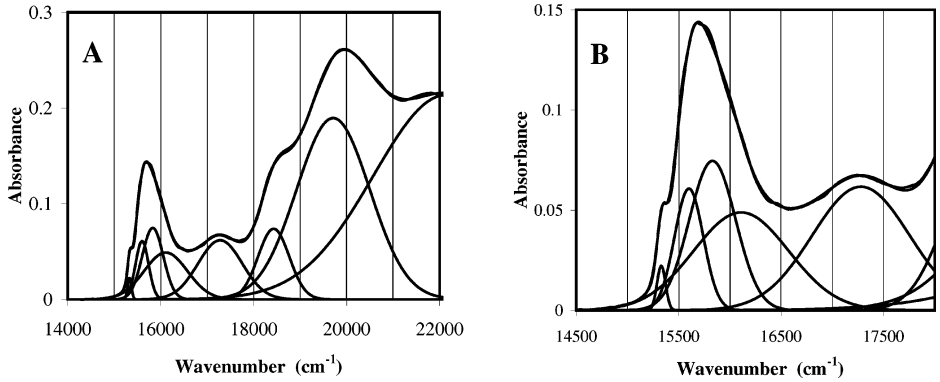


**Figure 12.** (A) Absorption spectrum of HRP with BHA in glycerol/water (60/40, v/v) pH 6 at 17 K. Gaussian function fits had the following respective position and widths (in $cm^{-1}$) and relative amplitudes: 15330, 41, 0.022; 15600, 140, 0.061; 15830, 227, 0.075; 16110, 465, 0.049; 17280, 476, 0.062; 18430, 336, 0.074; 19710, 787, 0.189; and 22150, 1570, 0.214. Top spectra are overlays of experimental spectrum and the sum of deconvolved peaks. Fit $r^2 = 0.9998$. (B) Same, but expanded scale.

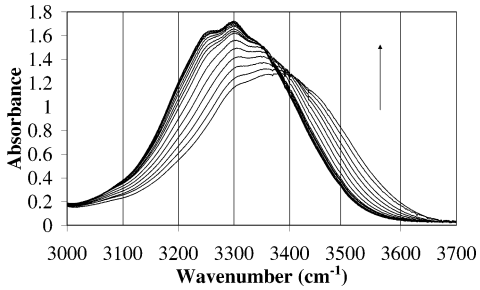


**Figure 13.** Temperature dependence of the OH stretch of a solution of $D_2O$/D-8 glycerol (60/40), 5 mM HRP and trace $H_2O$. pD ~ 6. Spacer was 100 $\mu$m. Temperature range: 290−15 K. The arrow is pointed toward the lowest temperature.

increasing and shifting to lower frequency for all absorption bands in the OH stretch region.

**Modeling of the Heme Environment.** The quantum calculations were undertaken to see what effect the presence of BHA would have on the Fe. The first case is without BHA and when the distal histidine, His42, is protonated. This situation would correspond to the pH of the experiment, pH 6.0. Our calculations show that the ground state has spin $^5/_2$ and the difference in energy between the spin state $^3/_2$ and $^5/_2$ is less than 4 kcal/mol. In the case of $S = {}^5/_2$ the oxygen $O_{water}$ of the water molecule in the distal side is 3.34 Å from the Fe. This finding is consistent with the 5-coordination of the Fe, which is suggested by the optical spectrum (Figure 2). The interaction of Fe−$H_2O$ is weak and the hydrogen bond between protonated His42 and water is strong, as indicated by its short distance: $His42N_\epsilon H_e{-}O_{water} = 1.92$ Å.

The calculations indicate that the substrate BHA screens the interaction between the distal His42 and the water molecule. The $Fe{-}O_{water}$ distance is now ~2.31 Å. The ground state is $^3/_2$. The difference in energy is ~6 kcal/mol when His42 is deprotonated and ~8 kcal/mol when His42 is protonated. The calculations are clear that BHA increases the stability of the spin state $^3/_2$ with respect to $^5/_2$. The short distance for $Fe{-}O_{water}$ suggests a 6-coordinated heme.

The charge on the iron changes in the presence of BHA. The Mulliken charge of Fe is 0.95 e in the absence of BHA, and increases to 1.2 e when BHA is present in the cavity. This indicates that more electrons are going to the heme.

## Discussion

The purpose of this work was to examine how a spectroscopic marker at the catalytic center of the enzyme is affected by surface conditions. The CT absorption band of heme proteins shows vibronic resolution, and hence resolution of the spectra is potentially a sensitive indicator of environment. Vibronic resolution of the CT band was evident from polarization of single crystals,[9] magnetic circular dichroism measurements,[36] and direct optical measurements shown in this paper and other works.[32,37] Vibrationally resolved spectra of charge-transfer bands have also been observed in porphyrin sandwich complexes.[38]

For HRP, at high temperature the CT absorption band is unresolved for all solvents, whereas at low temperature resolution is evident (Figures 4 and 8 and Table 2). The resolution of the CT absorbance band has a "memory" of the temperature that the glass was formed. The lines widths observed at low temperature are broader in the glass formed at high temperature. The lines become quite sharp in the solvent that is free to relax at low temperature, namely glycerol/water, and the lowest energy band has a width of about 100 $cm^{-1}$ fwhm. This corresponds to an excited-state lifetime of about 50 fs. Because the sample is still likely to be inhomogeneously broadened and the instrument resolution convolutes the observed line, the actual lifetime is expected to be longer than this. The bandwidth is comparable in width to the inhomogeneous bandwidths of porphyrin electronic transitions in heme proteins.[39,40]

We can separate various effects of the matrix on the protein: The solvent can restrict some motions of the protein, but at the same time allow others. The glycerol/water sample is fluid at high temperature and only forms a glass at low temperature. As temperature decreases, the viscosity increases and the solvent can have a greater influence on large amplitude motions. Finally, the solvent undergoes a glass transition, and the frequencies of the large-scale motions decrease. The sugar glass is prepared at high temperature, and therefore it is reasonable that conformational fluctuations arising from large-scale motions are locked in when the glass is formed. For this reason, at low temperature the optical spectrum is expected to be more inhomogeneously broadened in the sugar glass than in glycerol/water. This is in fact observed (compare Figure 4 with 6, and Figure 8 with 10). The fitted line widths also indicate narrower bands for absorption of HRP in glycerol/water relative to the sugar glass (Table 2).

In contrast to restrictions of some motions, the solvent can also allow other motions. Some of these motions may arise from internal protein motions that are independent of solvent. As an example, in cytochrome *c*, motions that are independent of solvent are a major contributor to the inhomogeneous broadening of the visible absorption bands.[14] For the heme the closest atomic contacts come from the surrounding polypeptide chain and

possible water molecules in the heme pocket. Some groups within the protein may have large dipolar moments but do not change with temperature. For instance, the amide groups of buried helixes do not change with temperature, as indicated by their IR absorption.[41,42] The largest effect on the temperature dependence of the optical transition will come from groups with large dipoles, and which are able to relax as the temperature decreases.

Because water is near the heme, we have to consider its effect on the CT band. Although the sugar glass is solid, IR evidence indicates that water within it retains motion. The bending and stretching modes of water in sugar glass shift over the entire temperature range from 10 to 300 K.[24,26] The motion of water molecules, with its large dipole moment, can potentially have a large effect on the spectra. The infrared spectrum gives some information on the water in the surrounding matrix. The water IR band changes continuously with temperature in glycerol/water (Figure 13). This is an indication of water mobility with rotational freedom in the solvent over the entire range. Because glycerol/water and hydrated sugar glass showed the same spectra, except for resolution, we can conclude that in both cases water is retained in the heme cavity. One of the intriguing aspects of solvent/protein interactions is the role of water mobility in allowing the protein to maintain motions. By extrapolation, one would expect that water in the heme pocket is also free to rearrange as temperature decreases.

The influence of water can be surmised when spectra of HRP without BHA in hydrated and desiccated sugar glasses are compared. For the protein at pH 6, the spectrum was sensitive to the presence of water. In glycerol/water and hydrated sugar film, the CT absorption spectra shifted to the blue as the temperature decreased (Figures 4 and 5). In the dry glass, the spectral shift did not occur (Figure 6). In contrast, in the sugar glass, when the internal site was blocked by the presence of BHA, the peak positions are the same when the sample is hydrated or dehydrated (Figures 9 and 10) and are the same as observed for the sample in glycerol/water (Figure 8). This is consistent with the view that BHA makes the heme pocket less accessible to the condition of the solvent. With BHA, there can either be no water present in the heme pocket, or else the bound water is rigidly held so that its dipole does not change with temperature.

The CT absorption band is stronger in the sample with BHA than without it (Table 1). Electron density changes at the heme occur due to the presence of BHA. This was shown for CO−HRP.[11] The present calculation on the charge and spin state of the Fe represents an advance in that a larger cluster was used in the calculation and the polarizability of the heme was taken into account. The calculations correctly predict spin state and coordination. The presence of BHA changes the Mulliken charge on the Fe. BHA allows the d orbitals of Fe to be closer to the $\pi$ orbitals of heme; this will enhance the CT absorption band.[15] Further work would be to calculate both ground- and excited-state parameters and then to derive the predicted spectra.

Here is a summary of the results: the charge-transfer band of HRP, arising from a transition involving both metal and porphyrin, is sensitive to the matrix conditions. At low temperature, the peaks are broader in sugar glass than in glycerol/water. This is consistent with the view that, when the glass is formed at high temperature, it traps a wide distribution of thermally activated forms, resulting in inhomogeneous broadening of the sample. When the channel is open, i.e., HRP in the absence of BHA, the CT absorbance band changes when the glass is dry or wet. Binding of the substrate increases the absorption of the CT band and increases the resolution. This suggests that addition of BHA shields the interior group from solvent conditions.

**Acknowledgment.** National Institutes of Health grant PO1 GM 48130 supported this work. A.D.K. thanks Dr. Judit Fidy for her support.

## References and Notes

(1) Gajhede, M. *Biochem. Soc. Trans.* **2001**, *29*, 91.
(2) Gajhede, M.; Schuller, D. J.; Henriksen, A.; Smith, A. T.; Poulos, T. L. *Nature Struct. Biol.* **1997**, *4*, 1032.
(3) Aitken, S. M.; Turnbull, J. L.; Percival, M. D.; English, A. M. *Biochemistry* **2001**, *40*, 13980.
(4) Schonbaum, G., R. *J. Biol. Chem.* **1973**, *248*, 502.
(5) Henriksen, A.; Schuller, D. J.; Meno, K.; Welinder, K. G.; Smith, A. T.; Gajhede, M. *Biochemistry* **1998**, *37*, 8054.
(6) Khajehpour, M.; Rietveld, I.; Vinogradov, S.; Prabhu, N. V.; Sharp, K. A.; Vanderkooi, J. M. *Proteins* **2003**, *53*, 656.
(7) Gouterman, M. *J. Mol. Spectrosc.* **1961**, *6*, 138.
(8) Eaton, W. E.; Hochstrasser, R. M. *J. Chem. Phys.* **1967**, *46*, 2533.
(9) Makinen, M. W.; Churg, A. K. Structural and analytical aspects of the electronic spectra of hemeproteins. In *Iron Porphyrins*; Lever, A. B. P., Gray, H. B., Eds.; Addison-Wesley: Reading MA, 1983; p 141.
(10) Jentzen, W.; Ma, J. G.; Shelnutt, J. A. *Biophys. J.* **1998**, *74*, 753.
(11) Kaposi, A. D.; Wright, W. W.; Fidy, J.; Stavrov, S. S.; Vanderkooi, J. M.; Rasnik, I. *Biochemistry* **2001**, *40*, 3483.
(12) Manas, E. S.; Vanderkooi, J. M.; Sharp, K. A. *J. Phys. Chem. B* **1999**, *103*, 6334.
(13) Manas, E. S.; Wright, W. W.; Sharp, K. A.; Friedrich, J.; Vanderkooi, J. M. *J. Phys. Chem. B* **2000**, *104*, 6932.
(14) Prabhu, N. V.; Dalosto, S. D.; Sharp, K. A.; Wright, W. W.; Vanderkooi, J. M. *J. Phys. Chem. B* **2002**, *106*, 5561.
(15) Stavrov, S. S. *Chem. Phys.* **2001**, *271*, 145.
(16) Leone, M.; Cupane, A.; Vitrano, E.; Cordone, L. *Biophys. Chem.* **1992**, *42*, 111; Huang, Q.; Szigeti, K.; Fidy, J.; Schweitzer-Stenner, R. *J. Phys. Chem. B* **2003**, *107*, 2822.
(17) Srajer, V.; Champion, P. M. *Biochemistry* **1991**, *30*, 7390.
(18) Douzou, P. *Cryobiochemistry. An Introduction*; Academic Press: London, 1977.
(19) Crowe, J. H.; Hoekstra, F. A.; Crowe, L. M. *Annu. Rev. Physiol.* **1992**, *54*, 579.
(20) Gottfried, D. S.; Peterson, E. S.; Sheikh, A. G.; Wang, J.; Yang, M.; Friedman, J. M. *J. Phys. Chem. B* **1996**, *100*, 12034.
(21) Cordone, L.; Galajda, P.; Vitrano, E.; Gassmann, A.; Ostermann, A.; Parak, F. *Eur. Biophys. J.* **1998**, *27*, 173.
(22) Khajehpour, M.; Troxler, T.; Vanderkooi, J. M. *Biochemistry* **2003**, *42*, 2672.
(23) Ponkratov, V. V.; Friedrich, J.; Vanderkooi, J. M. *J. Chem. Phys.* **2002**, *117*, 4594.
(24) Wright, W. W.; Guffanti, G.; Vanderkooi, J. M. *Biophys. J.* **2003**, *85*, 1980.
(25) Paul, K. G. *Acta Chem. Scand. B* **1958**, *12*, 1312.
(26) Wright, W. W.; Baez, C. J.; Vanderkooi, J. M. *Anal. Biochem.* **2002**, *307*, 167.
(27) Gilson, M.; Sharp, K. A.; Honig, B. *J. Comput. Chem.* **1988**, 327.
(28) Jayaram, B.; Sharp, K. A.; Honig, B. *Biopolymers* **1989**, *28*, 975.
(29) Nicholls, A.; Honig, B. **1991**, *12*, 435. Au: give title of journal for ref 29
(30) Nicholls, A.; Sharp, K. A.; Honig, B. *Proteins* **1991**, *11*, 281.
(31) Philipp, D. M.; Friesner, R. A. *J. Comput. Chem.* **1999**, *20*, 1468.
(32) Indiani, C.; Feis, A.; Howes, B. D.; Marzocchi, M. P.; Smulevich, G. *J. Am. Chem. Soc.* **2000**, *122*, 7368.
(33) Teraoka, J.; Kitagawa, T. *J. Biol. Chem.* **1981**, *256*, 3939.
(34) Kitagawa, T.; Hashimoto, S.; Teraoka, J.; Nakamura, H.; Yajima, H.; Hosoya, T. *Biochemistry* **1983**, *22*, 2788.
(35) Smulevich, G.; English, A. M.; Mantini, A. R.; Marzocchi, M. P. *Biochemistry* **1991**, *30*, 772.
(36) Sutherland, J. C.; Klein, M. P. *J. Chem. Phys.* **1972**, *51*, 75.
(37) Huang, Q.; Szigeti, K.; Fidy, J.; Schweitzer-Stenner, R. *J. Phys. Chem. B.* **2003**, *107*, 2822.
(38) Perng, J.-H.; Duchowski, J. K.; Bocian, D. F. *J. Phys. Chem.* **1990**, *94*, 6684.
(39) Fidy, J.; Laberge, M.; Kaposi, A. D.; Vanderkooi, J. M. *Biochim. Biophys. Acta* **1998**, *1386*, 331.
(40) Kaposi, A. D.; Wright, W. W.; Vanderkooi, J. M. *J. Fluorescence* **2003**, *13*, 59.
(41) Kaposi, A. D.; Fidy, J.; Manas, E. S.; Vanderkooi, J. M.; Wright, W. W. *Biochim. Biophys. Acta* **1999**, *1435*, 41.
(42) Manas, E. S.; Getahun, Z.; Wright, W. W.; DeGrado, W. F.; Vanderkooi, J. M. *J. Am. Chem. Soc.* **2000**, *122*, 9883.